

Manufacturing cellular materials via three-dimensional printing of spray-dried metal oxide ceramic powder

C.B. Williams & D.W. Rosen

Georgia Institute of Technology, Atlanta, Georgia, United States

ABSTRACT: Cellular materials, metallic bodies with gaseous voids, are a promising class of materials that offer high strength accompanied by a relatively low mass. Unfortunately, existing manufacturing techniques constrain a designer to a predetermined part mesostructure, material type, and macrostructure. In this paper, the authors document their design rationale for the selection of the Three-Dimensional Printing (3DP) additive manufacturing process as a means to fabricate metallic cellular materials. This is achieved by selectively printing a solvent into a bed of spray-dried metal oxide ceramic powder. The resulting green part undergoes reduction and sintering post-production processes in order to chemically convert it to metal.

1 MANUFACTURING CELLULAR MATERIALS

1.1 Cellular materials

Low-density cellular materials are a special classification of metallic structures which have gaseous voids dispersed throughout the material [1]. This special class of materials features a metallic phase that divides space into closed cells (in the range of 0.1 to 10 mm) which contain the gaseous phase. These voids reduce the part density while improving the part strength, impact-absorption, and both thermal and acoustic insulation. Unfortunately, existing cellular material manufacturing techniques constrain a designer to a predetermined part mesostructure, material type, and macrostructure [2].

1.2 Additive manufacturing of cellular materials

Layer-based additive manufacturing (AM) offers the utmost geometrical freedom in the design and manufacturing of a part. As such, many researchers have recently explored the use of AM as a means of producing cellular materials.

Several indirect approaches to manufacturing cellular materials with AM have been proposed (e.g., using AM to create a tool for casting) [3,4]. Such approaches tend to be expensive, and the resulting parts are plagued by porosity due to the inability of the fill material to access all of the features of the complex geometry [5]. As a consequence, the geometry of the part (the diameter of trusses and the angles between them) must be carefully designed to

fit within the constraints of the manufacturing process.

Due to these limitations, researchers have turned their attention to directly manufacturing cellular materials through AM. Direct approaches with conventional rapid prototyping technologies (e.g., stereolithography [6] and selective laser sintering [7]) have been successful, but are constrained by their limited selection of working materials. As such, many have investigated direct-metal AM approaches as a means of creating cellular materials.

As described in [2], the majority of direct-metal AM approaches are generally not ideal for manufacturing cellular materials due to limitations from poor resolution, poor surface finish, poor material properties, limited material selection, and need for support structures. Selective Laser Melting [8], Direct Metal Laser Sintering [9], and Electron Beam Melting [10] have had some success with creating cellular materials; however, they suffer from limitations (e.g., high cost, limited build rate, need for support structure to prevent warping and curling, arduous removal of pre-sintered support powder, etc.) that provide opportunity for further investigation and potential improvement.

1.3 Context: Designing an additive manufacturing process for the realization of cellular materials

The authors' are driven by the notion of a manufacturing process that would provide sufficient flexibility so as to empower a designer to create an ideal cellular mesostructure for the (multiple) design goal(s) specific to a part's application. In this paper,

the authors document progress towards creating a manufacturing process that can create three-dimensional, low-density cellular metal parts with designed mesostructure. Specifically, the authors have augmented the three-dimensional printing process (3DP) for the creation of green parts (formed from metal oxide powders) that are suitable for conversion to metal via thermal chemical post-processing.

The reduction and sintering post-process, a feature of the manufacturing process for the realization of linear cellular honeycombs, is described in Section 2. In Section 3 the authors present their rationale for the selection and augmentation of the 3DP process through a functional analysis of additive manufacturing processes. Preliminary results are provided in Section 4 along with closing comments in Section 5.

2 REDUCTION OF METAL OXIDES TO CREATE METAL CELLULAR MATERIALS

In an effort to address the limitations found in the creation of cellular materials via direct-metal AM technologies, the authors look to other processes as a means of creating metallic parts. Specifically they look to the Georgia Tech Lightweight Structures group's work in creating metallic linear cellular alloys (LCA) from metal oxide precursors.

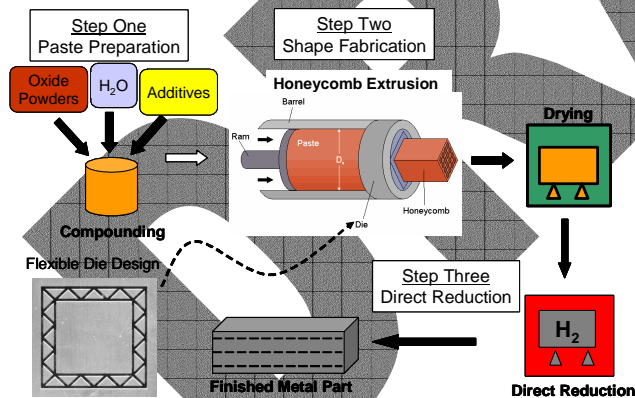


Figure 1. Linear cellular alloy manufacturing process [11].

The process (illustrated in Figure 1) begins with a metal oxide-based ceramic paste (containing lubricants, binders, and other additives) that is extruded through an interchangeable die (at room temperature). The ceramic green body is then dried, and processed in a reducing atmosphere to chemically convert the precursor into a metallic artifact [12]. The reducing agent (e.g., hydrogen or carbon monoxide gas) reacts with the oxygen atoms of the metal oxide powder and forms water vapor, which is then removed from the system.

A wide variety of materials can be processed with this reduction technique. The primary requirement

is that a metal oxide must be reducible at moderate temperatures (below the melting points of the materials involved) with a partial pressure of oxygen no lower than 10-16 atm. Unfortunately some elements such as Ti and Al are stable under these conditions; hence, they cannot be introduced into the alloy as an oxide, and must be added in a secondary process. With this technique, Cochran and coauthors have successfully processed a number of transition metal oxides (Fe, Ni, Co, Cr, N Cu, Mo, W, Mn, and Nb), as well as many engineering alloys including stainless steel, maraging steel, Inconel, and Super Invar [13]. Through metallurgical characterization Cochran and coauthors have demonstrated that “the direct reduction metal is comparable to conventionally processed counterparts” [11]. Copper parts have demonstrated high thermal conductivity, and high strength and energy absorption have been demonstrated for maraging steel cellular structures.

Cell sizes in the range of 0.5 to 2.0 mm with web thicknesses of 50 to 300 μm have been fabricated with this process [11]. These small features are accomplished, in part, by the shrinkage (and large increase in density) that is accompanied with the reduction process. Shrinkage is typically on the order of 30 to 70% by volume; this can be advantageous when fine geometric features are desired that would otherwise would be difficult or expensive to fabricate [13]. It is important to note that this large amount of shrinkage can cause cracks, laminations, disruption of dimensional stability, and/or warping if not controlled carefully [12].

Chemical reduction of metal oxide green parts to metal has the potential to alleviate many of the limitations found in direct-metal AM of cellular materials. An implementation of this post-processing technique is economically efficient, as the cost differential between a metal oxide powder and its metal counterpart is usually better than a 1-to-10 ratio [13]. Fine oxide powders are readily available in a pure and stable form. Compared to pure metal powders, metal oxides are safer as they are neither carcinogenic nor explosive.

It is important to note that while a wide-range of geometries can be theoretically made using this process, the structure must be open for the article to survive the conversion process and emerge as a monolithic product. In general, the requirement for the geometry is to have a high surface-to-volume ratio and a highly open access to the interior. Multiple openings provide an unrestricted passage of both the reducing agents (hydrogen) to and the reaction products (water) from the interior [12]. It is also important that the structure does not have a widely varied thickness throughout its cross-section; an equal coercion force in the structure is needed so that it will survive the large shrinkage that takes place in the reduction process [13].

3 FUNCTIONAL ANALYSIS OF ADDITIVE MANUFACTURING PROCESSES FOR THE REALIZATION OF CELLULAR MATERIAL

Having decided to combine additive manufacturing with reduction post-processing, the authors are faced with the following task: to design a layer-based AM process that is capable of creating green cellular parts composed of metal oxide ceramic material that are suitable for thermal chemical post-processing. Following a systematic conceptual design and preliminary selection process, the authors identified three AM processes that would be appropriate for the fabrication of ceramic cellular materials: direct aqueous inkjet printing, direct hot-melt inkjet printing, extrusion, and three-dimensional printing [14].

Through systematic evaluation, the authors identified (an augmented) three-dimensional printing process as the most appropriate manner of creating green cellular ceramic parts. In this section the rationale for this design decision is documented in the context of a functional analysis of existing AM processes.

3.1 Additive manufacturing morphological matrix

From an abstract view, each AM process is comprised of the same five functions: store material, pattern energy/material, provide energy, provide new material, and provide support. These functions are presented along with various embodying working principles in Figure 2 (a morphological matrix [15]).

		Solutions						
Sub-Functions	Store Material	Powder	Two Phase Powder	Powder Coated w/ Binder	Powder / Binder Suspension	Wire / Rod	Gas	Tape / Sheet
	Pattern	Material (1D)	Energy (1D)	Both (1D)	Material (2D)	Energy (2D)	Both (2D)	
	Provide Energy	Sinter	Melt	Bind	Evaporate	Cut	Chem. Reaction	Photo-polymerize
	Provide New Material		Recoat by Spreading	Recoat by Spraying	Recoat by Dipping	Recoat by Layer	Direct Material Addition	
	Support	5-axis Deposition	Material Bed	Breakable Support Material	Thin Trusses of Build Material	Dissolvable Support Material	Organic Support Material	No Support

Figure 2. Morphological matrix for three-dimensional printing of spray-dried metal oxide powder

By choosing a working principle from each function, one can outline the general form of almost all of the existing AM processes. As an example, the solution principle for the augmented 3DP process proposed in this paper is shown in Figure 2. In this concept, a solvent is selectively printed over a bed of spray-dried ceramic powder via a series of inkjet printing nozzles. The solvent dissolves the binder that coats the spray-dried granules, thus binding them together. Additional layers of powder are spread across the powder bed by a rolling mechanism. Green parts are then subjected to a thermal

chemical post-production process wherein the polymer binder is decomposed and the ceramic powder is reduced and sintered.

3.2 Store material

The function labeled “store material” represents how the raw material for the building of the part is stored before being processed. Generally, the working principles listed for this function (Figure 2) do not have a direct impact on the ability of an AM process to manufacture cellular materials.

The primary concern in the AM of ceramics is in creating a green part with a sufficient solids loading percentage for it to be suitable for sintering and reduction (i.e., to easily reach full density and to minimize warping, curling, and shrinkage). This is especially important in technologies that rely on powder/binder suspensions (direct inkjet printing, extrusion, and stereolithography) as there is a physical limit to the amount of powder that can be introduced into the suspension before it is too viscous to be processed. For example, Derby and coauthors have only been able to successfully inkjet print suspensions of ceramic powder in a thermoplastic polymer that contain ~35 vol.% solids [16]. Inkjet printing of aqueous ceramic suspensions has reached a maximum of only 15 vol.% [17]. Without the need to form droplets, extrusion techniques have processed slurries with ~40 vol.% ceramics (maximum of ~55 vol.%) [18,19]. The use of powder/binder suspensions is further hampered by the amount of effort that is required to adequately suspend the ceramic powder in the solution. Not only does successful suspension require extensive experimentation and knowledge of materials engineering and chemistry, but the solution is unique to each material that the AM technique will process. Taking all of these limitations into account, it is difficult to recommend the use of powder/binder suspensions for the “store material” function.

Working with a powder form of the raw material seems to be a more appropriate working principle for the manufacture of cellular materials. If used in a powder bed, the maximum solids loading of the green part is no longer a function of rheology of a suspension; instead, it is a function of the tap density of the powder (dependent on particle size and shape). Utela and coauthors report powder beds with as high as 55 vol% in their work with 3DP [20].

Research involving the 3DP of ceramics encountered early setbacks because of the use of single-phase ceramic powders. The fine powders needed for high powder bed density and good sintering characteristics did not flow well enough during the recoating process to spread into defect-free layers [21]. As a result, larger powder sizes were used, resulting in green parts featuring only 35% solids loading [21].

As such, research on ceramic 3DP shifted to the use of a slurry-based working material (S-3DP). In this approach, layers are first deposited by ink-jet printing a layer of slurry over the build area (“powder/binder suspension” working principle). Once the slurry dries, binder is selectively printed to define the part shape. This is repeated for each individual layer, increasing build time dramatically [22]. Alumina, and silicon nitride have been processed with this technique, improving green part density to 67%, and utilizing layer thicknesses as small as 10 μm [23]. In fact, Kernan and coauthors used the combination of S-3DP and the reduction post-process described in Section 2 to process tungsten carbide-cobalt samples from a tungsten carbide mixture [24]. Unfortunately, the requirement of a high packing density of the powder bed opposes the requirement of efficient separation of the finished part from the unpatterned material [25]. The redispersion post-processing of S-3DP parts typically features “audible explosions” from the pressure built-up from entrapped air in the part. As such, the delicate features characteristic of cellular materials are almost impossible to salvage in parts created via S-3DP.

To address these limitations, the authors propose the use of spray-dried granules (“powder coated with binder” working principle). Spray drying is the process of spraying a slurry composed of fine powder particles and a binder into a warm drying medium to produce powder granules that are relatively homogeneous [26]. The use of spray-dried granules make it possible to work with fine particles (~60 vol.%, 1 – 5 μm ceramic particles per granule) thus improving sintering, decreasing porosity, and decreasing grain size in the finished part. While the porous nature of spray-dried powders is detrimental in that it slightly decreases the solids loading possible for a green part, it is beneficial for the manufacture of cellular materials since smaller printed primitives result from the increased absorption of the jetted binder [22]. Furthermore, spray-dried granules are nearly spherical and typically on the order of 30 μm in diameter, therefore they flow very well and are easily recoated in the 3DP process [27].

The final powder-based working principle, “two phase powder,” has been implemented by Utela and coauthors [20]. Specifically, they combine powdered acetate alumoxane with powdered alumina in a 3DP powder bed and activate the in-bed binder by selectively printing a mixture of water and isopropanol. While both techniques are capable of producing high quality green parts, Beaman and coauthors note that working with binder-coated particles is preferred over simply mixing the two materials since mixed materials can segregate by density and could potentially lead to highly variable powder and part properties [28]. Furthermore, in Selective Laser Sintering, the strength of green parts made from coated particles are usually higher than that of parts made

using a powder mixture at the same polymer content [29].

3.3 Pattern

The “pattern” function captures the act of selectively depositing (or patterning) material and/or energy to create the final part. The working principles are categorized by their dimension of deposition.

One-dimensional patterning refers to those processes that have single point material deposition methods such as extrusion (e.g., fused deposition modeling [30], multi-jet solidification [31], robocasting [32], extrusion free-forming [19], etc.) or laser-based energy deposition methods (e.g., stereolithography [33], electron beam melting [34], selective laser sintering [35], selective laser melting [36], and laser chemical vapor deposition [37]). The Laser Engineered Net Shaping process, which features selective laser cladding, is an example of a process with both energy and material patterning in one dimension [38]. The speed of patterning found in one dimensional processes is constrained by the fundamental limit of the machines’ scanning speed. It is simply not possible to scan a single deposition spot fast enough to be economically competitive with traditional manufacturing technologies.

Two-dimensional patterning techniques do not suffer from this limitation as they entail processes that are able to pattern large portions of a cross-section in one motion. This can include the delivery of energy through a mask (e.g., mask-based stereolithography [39], high speed sintering [40]), the patterning of large portions of material (e.g., layered object manufacturing [41]), and even printing methods (e.g., inkjet printing [42,43], and three-dimensional printing) which feature several parallel one-dimensional depositions of material or binder. Electrostatic printing [44] and ultrasonic consolidation [45] are examples of processes that pattern both energy and material in two-dimensions. Two-dimensional patterning processes are preferred for manufacturing not only because of the aforementioned concerns regarding process throughput, but also because they are capable of being scaled cost effectively since they do not require an expensive laser element [46].

Specific to the realization of cellular materials, it is imperative that a process must be able to pattern the small features typical of cellular materials. With cell sizes in the range of 0.5 – 2 mm and wall thicknesses as small as 200 μm , cellular materials require an AM process with high deposition accuracy (± 0.05 mm), high z-resolution (≤ 0.1 mm), and small minimum feature size (≤ 0.2 mm).

In addition to these quantitative requirements, the patterning process must be able to effectively create the cross-sections typical of cellular materials. Three representative cellular material geometries are

presented below (Figures 3-5a): a chiral honeycomb structure (wall thickness = 1.5 mm), a swept cellular matrix (wall thickness = 1.5 mm; cell size = 2.25 mm), and a trussed structure (truss diameter = 1.5 mm). Characteristic cross-sections of each type of cellular material are also shown for both principal build directions.

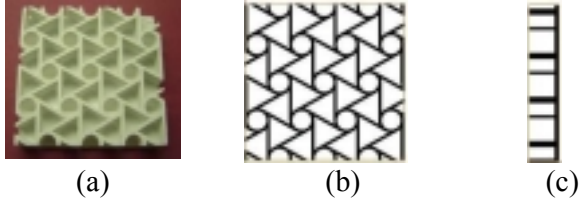


Figure 3. Cross-section of chiral honeycomb; (a) as built, (b) x-y orientation, (c) y-z orientation.

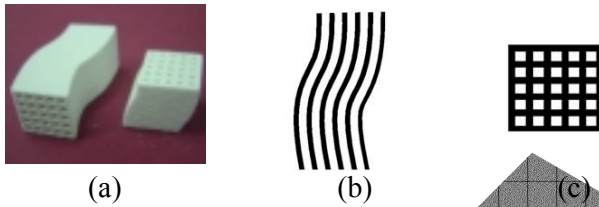


Figure 4. Cross-section of swept periodic cellular material; (a) as built, (b) x-y orientation, (c) y-z orientation.

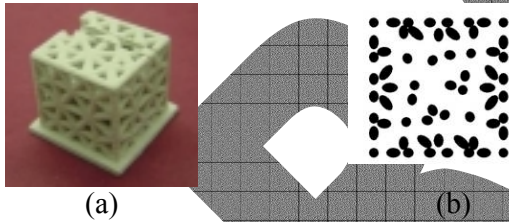


Figure 5. Cross-section of trussed cube; (a) as built, (b) x-y orientation.

The cross-sections of the periodic cellular structures shown in Figure 3 and 4 are composed of continuous lines and are relatively easy to create with almost any patterning process. The same is not true of the trussed cube (Figure 5) however, as it requires very small discrete depositions of energy and/or material. As shown in Figure 6, those trusses angled with the slicing plane have an elliptical cross-section (assuming a cylindrical truss with constant diameter, d).

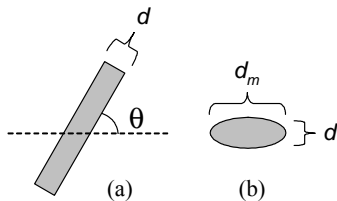


Figure 6. Elliptical cross-section of cellular truss structure

The minor axis of the ellipse is d , and the major axis of the ellipse, d_m , can be calculated as:

$$d_m = d / (\cos(90 - \theta)) \quad (1)$$

where θ is the angle of the truss relative to the slicing plane.

This type of small, discrete deposition is extremely difficult to achieve with extrusion-based processes because they are not suited for the start-stop motions needed for point-like depositions. This is especially true when extruding viscous slurries with a high volume fraction of solids. Work towards producing cellular materials with extrusion processes have been limited to periodic lattice structures created by a serpentine motion (referred as “log-piles” in [19]) as shown in [18] and [47]. In addition, sharp edges are filleted because the material is yielded behind the extrusion nozzle. Finally, parts created by extrusion processes are typically porous due to poor optimization of material flow, filament/roller slippage, liquefier head motion, and build/fill strategies (i.e., the tool path prevents the road depositions from completely meshing with the cross-section’s boundary contours - referred to as subperimeter voids [48]).

AM processes that pattern material via inkjet printing can efficiently create all three of cross-sections presented above due to the selective deposition of small droplets of material ($\sim 75 \mu\text{m}$). Three-dimensional printing (used to create the parts shown in Figures 3-5a) and direct hot-melt inkjet printing can create features as small as $100 \mu\text{m}$ with $100 \mu\text{m}$ layer thicknesses [16,49]. Furthermore, it is possible that even smaller features will be able to be obtained due to the large shrinkage that takes place during the reduction and sintering post-processes described in Section 2.

3.4 Provide energy

This function describes the need for a delivery of some form of energy to transform, shape, or change the phase of the raw material to obtain the desired part. While most working principles presented for this sub-function (Figure 2) do not directly limit the manufacture of cellular materials, some are more preferred than others.

Photo-polymerization, found in stereolithography, is not a feasible means of processing most ceramics. Polymerization typically cannot occur since the solid particles in the powder/resin suspension reflect the UV radiation and thus prevent the resin from absorbing enough energy to surpass its critical exposure level. As such, only those ceramics which have refractive indexes close to that of the resin are able to be processed (e.g., alumina, silica, and PZT [50,33]).

The sintering working principle features two types of sintering: solid state sintering (SSS; the use of high temperature to initiate diffusion and necking between ceramic particles) and liquid phase sintering (LPS; the joining of two ceramic particles by melting/fusing a secondary binder material). A wide variety of materials can be processed with SSS, but the process is slow and a post-sintering operation is required to improve part characteristics [7]. LPS is favored over SSS for the proposed manufacturing process chain since it produces a green part suitable for post-processing in a reducing atmosphere. Generally speaking, however, neither “sintering” nor “melting” are preferred working principles since heat affected zones caused by thermal processing are difficult to control, which can result in non-uniform depositions, warping, and residual stresses in the final part [51].

In direct aqueous inkjet printing, deposition of material occurs by evaporating the solvent from a printed droplet of a dilute (5-14 vol.%) ceramic suspension [43]. While green parts created by this process typically have a volume fraction of 60%, the low solids content of each individual deposition results in layer thicknesses as small as $0.7\ \mu\text{m}$ [52]. Not only is this process extremely slow (each layer must be thoroughly dried by a hot-air blower for up to 20 seconds), but no depositions of over 1 mm in height have been reported [52].

As stated in Section 3.2, the authors have chosen to work with spray-dried metal oxide powders as a means of processing fine particles. An additional advantage in using spray-dried particles is that the binder used to form granules can be activated in the powder bed, thus eliminating the need for printing a polymeric binder. Specifically, the authors have chosen to spray dry metal oxide ceramic particles with a water soluble poly-vinyl alcohol (PVA). Thus, in order to form a deposit, all that is required is printing of an aqueous solution into the powder bed. This solution activates the PVA that coats the particles, which causes the granules to deform and to form necks with one another. This decreases the distances between individual ceramic particles, which improves the sintering characteristics of the green part. PVA was chosen as the binder because it is (i) a common binder that works well with almost an oxide ceramic, (ii) soluble in water, and (iii) the resulting parts have considerable strength and are handled easily in the green form [53]. Perhaps most important in this “binding” working principle is that it is modular – all PVA spray-dried granules will behave the same with the solvent, regardless of the ceramic material chosen as the core powder. As such, there is no requirement for individualized binder formulation or powder/binder suspension.

3.5 Provide new material & support

In the context of using AM to fabricate cellular materials, the sub-functions “provide new material” (the manner in which new layers of material are supplied to the process) and “provide support” (the manner in which deposited material and overhanging geometry are stabilized) are somewhat coupled. The complex internal geometry of cellular materials prohibits the use of an AM technique that constructs support structure that must be manually removed (e.g., the fibrous supports built during stereolithography).

Although the use of a powder bed eliminates the need for support structures as the un-patterned powder can support complex geometry, the un-patterned material can be trapped, or at the least, be very troublesome to remove with specific cellular geometries (e.g., microchannels found in cellular honeycombs, skinned cellular structures, etc.). Therefore, the most appropriate way for the internal voids found in cellular materials to be realized in an AM process is to construct support structures with a separate dissolvable or pyrolyzable material (or through processing self-support material as seen in the extrusion of colloidal ceramic gels [47]). Examples include Stratasys’ WaterWorks™ water soluble support materials for its extrusion process [54] and Mott and coauthors’ use of a carbon suspension as a fugitive mechanical support in aqueous direct inkjet printing [55]. Since selective deposition of different materials can only be achieved with direct material addition, this “provide new material” working principle is preferred over those that involve recoating.

Unfortunately, as discussed in Sections 3.2 and 3.3, direct material addition is not a preferred method of additively manufacturing ceramics due to difficulties in patterning viscous powder/binder suspensions. As such, the authors make a compromise by selecting the working principle of recoating a powder bed through spreading featured in 3DP. While this may place a limit on the size of voids and will prohibit the construction of closed cells, it is believed that the use of highly-flowable spray-dried powder will minimize the difficulties in removing un-patterned powder.

4 PRELIMINARY RESULTS

Preliminary experimentation with the proposed process featured two phases: (i) creation of alumina green parts followed by sintering and (ii) creation of maraging steel parts through the processing of metal oxide powder mixture.

4.1 Alumina

In this first phase of experimentation, spray-dried granules of alumina particles and a water-soluble PVA binder were tested. Two different powder diameters, 100 μm and 40 μm were used.

The solubility of the PVA binder that coats the ceramic particles was explored first. Droplets of distilled water, ZCorp ZP7 binder, and ethyl alcohol were manually deposited (10 μL ; ~ 2.7 mm diameter) onto small beds of the spray-dried powder. Significant granule deformation was observed as the binder dissolved and necking between the granules occurred. This can be seen in Figure 7 – the right-hand side of the figure shows loose granules; the left-hand side of the figure shows the solid primitive. Each solvent tested was able to sufficiently dissolve the PVA and create a solid primitive suitable for easy removal from the surrounding unbound powder.



Figure 7. Spray-dried powder deformation

Confident that the spray-dried granules could be easily bound together with selective deposition of water droplets, the ability of the spray-dried powder to be recoated was tested. The experiments were conducted using a ZCorp Z402 3DP machine. As expected, the 100 μm diameter granules were too large for even the largest layer thickness setting (0.18 mm). As such, layers exposed to patterned solvent were swept away during recoating. Working with smaller granules (≤ 40 μm in diameter; obtained by sieving 100 μm powder) alleviated this problem. These smaller granules recoated well with no visible surface defects.

Finally, test samples featuring chiral honeycomb topology (Figure 3b) were successfully fabricated from the 40 μm diameter granules using water as a solvent in the spray-dried powder bed. 25 layers were printed at a layer thickness of 0.09 mm with little process optimization. The resulting green parts were extremely fragile, suggesting that the binder coating was not sufficiently dissolved. The samples were then sintered using the following three-step heating cycle:

- i. ramp to 500 $^{\circ}\text{C}$ at 2 $^{\circ}\text{C}/\text{min}$ to burn out binder

- ii. ramp to 1600 $^{\circ}\text{C}$ (at 3 $^{\circ}\text{C}/\text{min}$) and hold for 6 hours to sinter
- iii. cool at 5 $^{\circ}\text{C}/\text{min}$

Since the base powder, alumina, is not reducible, the reduction process was not attempted with these samples.

The resulting ceramic part (Figure 8) showed no visible cracking or curling. The samples had an average relative density of 65% (as determined by the Archimedes method). A 20% linear shrinkage was also observed.

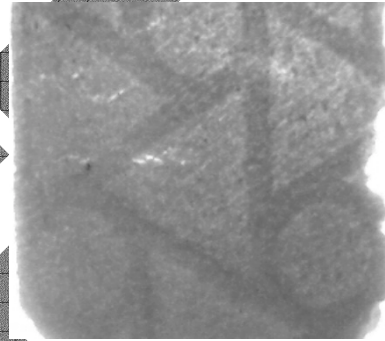


Figure 8. Ceramic chiral pattern produced by 3DP

4.2 Maraging Steel

In order to test the reduction phase of the post-process, the authors shifted their focus to a material system that was reducible. A metal oxide powder system that will chemically convert to maraging steel upon reduction was created by combining iron oxide (Fe_3O_4), nickel oxide (NiO), cobalt oxide (Co_3O_4), and molybdenum metal (Mo). These powders were mixed together via ball milling for 24 hours. Once combined, the resulting powder was spray-dried with PVA to form granules with a mean diameter of 30 μm .

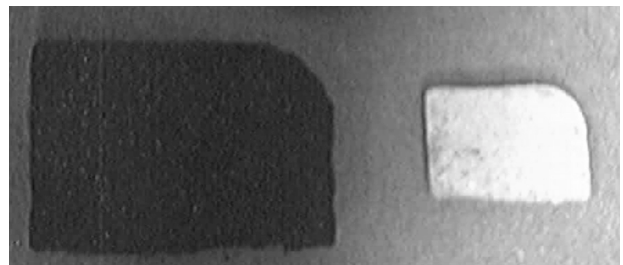


Figure 9. Maraging steel coupons produced by 3DP; (LHS) green part, (RHS) as sintered and reduced

Sample coupons were created with a ZCorp Z402 3DP machine using the ZCorp ZP7 binder. In their green form, the samples were 20 mm x 20 mm x 2.5 mm (LHS of Figure 9). The samples were then reduced and sintered in a 10% H_2 / 90% Ar environment using the following four-step cycle:

- i. ramp to 450 $^{\circ}\text{C}$ at 2 $^{\circ}\text{C}/\text{min}$ to burn out binder

- ii. ramp to 850 °C (at 3 °C/min) and hold for 6 hours for reduction of the sample
- iii. ramp to 1300 °C (at 3 °C/min) and hold for 3 hours to sinter the sample
- iv. cool at 5 °C/min

The resulting metal parts (RHS of Figure 9) had an average relative density of 70% and a 46% linear shrinkage. The large shrinkage is due to the low solids loading of the green part and the removal of the relatively large oxygen atoms through reduction. The authors anticipate a higher relative density from future tests via better dissolving of the binder coating of the spray-dried granules (thus bringing the oxide powder particles into closer contact), optimization of the 3DP process, and through a more aggressive sintering cycle.

5 CLOSURE

In this paper the authors present a layer-based additive manufacturing process for the realization of metal parts of designed mesostructure. Specifically, they detail a manufacturing process that features the three-dimensional printing of spray-dried metal oxide ceramic powders and a post-production process wherein the green part is sintered and reduced to metal in a hydrogen atmosphere, thus chemically converting the green part to metal.

The rationale for the design of this process is presented through an analysis of existing additive manufacturing techniques at the functional level. It was shown that three-dimensional printing (3DP) is most appropriate for the realization of cellular materials because of its speed, cost effectiveness, scalability, high resolution, and use of a powder bed for supporting overhanging features.

Furthermore, the authors propose to augment the existing 3DP process through the use of spray-dried granules in the powder bed. Selectively printing solvent into a bed of spray-dried granules activates the binder which coats the particles, thus binding them together to form a green part. Doing so “modularizes” the typically complex binder/powder interaction – the core powder material can be changed without altering the printed solvent as long as it is spray-dried with the same binder. Furthermore, spray-dried powders enable the processing of fine ceramic particles with 3DP, thus improving sintering mechanics and reducing grain size.

Future work on this process is focused in improving the density of the green part. As such, the authors are investigating printing a suspension of solvent and metal oxide nanoparticles into the powder bed as a means of increasing part density and, consequently, reducing shrinkage during post-processing as shown in [20] and [56].

Finally, a high-level contribution of this paper is the documentation of a systematic design process of

an additive manufacturing technology. The design endeavor presented in this paper is unique in that it is driven by the unique requirements of manufacturing cellular material geometries. In this context, learning opportunities arise from the systematic analysis of the characteristics of the principal solutions found in additive manufacturing.

ACKNOWLEDGEMENTS

We gratefully acknowledge the funding given by NSF DMI-0522382. Christopher Williams acknowledges the financial support provided by the Georgia Tech Technological Innovation: Generating Economic Results (TI:GER) program (NSF IGERT-0221600). Very special thanks are offered to Dr. Joe Cochran in the Materials Science and Engineering Department of Georgia Tech for sharing his wealth of knowledge and insight into the reduction and sintering post-process. The authors would also like to thank the generosity of Mr. Joe Pechin of Aero-Instant Spray Drying Services for his assistance in preparing the experimental powder system.

REFERENCES

1. Banhart, J., 2000, "Manufacturing Routes for Metallic Foams," *The Member Journal of the Minerals, Metals & Materials Society*, Vol. 52, No. 12, pp. 22-27.
2. Williams, C. B., F. M. Mistree and D. W. Rosen, 2005, "Investigation of Solid Freeform Fabrication Processes for the Manufacture of Parts with Designed Mesostructure," *ASME IDETC Design for Manufacturing and the Life Cycle Conference*, Long Beach, California, DETC2005/DFMLC-84832.
3. Hattiangadi, A. and A. Bandyopadhyay, 1999, "Processing, Characterization and Modeling of Non-Random Porous Ceramic Structures," *Solid Freeform Fabrication Symposium*, Austin, TX, pp. 319-326.
4. Chiras, S., D. R. Mumm, A. G. Evans, N. Wicks, J. W. Hutchinson, K. Dharmasena, H. N. G. Wadley and S. Fichter, 2002, "The Structural Performance of Near-Optimized Truss Core Panels," *International Journal of Solids and Structures*, Vol. 39, pp. 4093-4115.
5. Wadley, H. N. G., 2002, "Cellular Metals Manufacturing," *Advanced Engineering Materials*, Vol. 4, No. 10, pp. 726-733.
6. Wang, H. and D. W. Rosen, 2002, "Parametric Modeling Method for Truss Structures," *ASME Computers and Information in Engineering Conference*, Montreal, CA, DETC2002/CIE-34466.
7. Kruth, J. P., P. Mercelis, L. Froyen and M. Rombouts, 2004, "Binding Mechanisms in Selective Laser Sintering and Selective Laser Melting," *Solid Freeform Fabrication Symposium*, Austin, TX., pp. 44-59.
8. Pham, D. T., S. S. Dimov, C. Ji and R. S. Gault, 2003, "Layer Manufacturing Processes: Technology Advances and Research Challenges," *1st International*

9. Agarwala, M., D. Bourell, J. Beaman, H. Marcus and J. Barlow, 1995, "Direct Selective Laser Sintering of Metals," *Rapid Prototyping Journal*, Vol. 1, No. 1, pp. 26-36.
10. Cansizoglu, O., D. Cormier, O. Harrysson, H. West and T. Mahale, 2006, "An Evaluation of Non-Stochastic Lattice Structures Fabricated Via Electron Beam Melting," *Solid Freeform Fabrication*, Austin, TX, pp. 209-2119.
11. Cochran, J. K., K. J. Lee, D. L. McDowell and T. H. Sanders, 2002, "Multifunctional Metallic Honeycombs by Thermal Chemical Processing," *Processing and Properties of Lightweight Cellular Metals and Structures (TMS)*, pp. 127-136.
12. Cochran, J. K., K. J. Lee and T. H. Sanders, 2003, "Metallic Articles Formed by Reduction of Nonmetallic Articles and Method of Producing Metallic Articles," US 6,582,651 B1, USA, Georgia Tech Research Corporation.
13. Cochran, J. K., K. J. Lee, D. McDowell, T. H. Sanders, B. Church, J. Clark, B. Dempsey, K. Hurysz, T. McCoy, J. Nadler, R. Oh, W. Seay and B. Shapiro, 2000, "Low Density Monolithic Metal Honeycombs by Thermal Chemical Processing," *Fourth Conference on Aerospace Materials, Processes, and Environmental Technology*, Huntsville, AL.
14. Williams, C. B., F. M. Mistree and D. W. Rosen, 2005, "Towards the Design of a Layer-Based Additive Manufacturing Process for the Realization of Metal Parts of Designed Mesosstructure," *16th Solid Freeform Fabrication Symposium*, Austin, TX.
15. Zwicky, F., 1967, "The Morphological Approach to Discovery, Invention, Research and Construction," *New Methods of Thought and Procedure*, (F. Zwicky and A. G. Wilson, eds.), Springer-Verlag, New York, pp. 273-297.
16. Seerden, K. A. M., N. Reis, J. R. G. Evans, P. S. Grant, J. W. Halloran and B. Derby, 2001, "Ink-Jet Printing of Wax-Based Alumina Suspensions," *Journal of the American Ceramic Society*, Vol. 84, No. 11, pp. 2514-2520.
17. Wright, M. J. and J. R. G. Evans, 1999, "Ceramic Deposition Using an Electromagnetic Jet Printer Station," *Journal of Materials Science Letters*, 18, pp. 99-101.
18. Lewis, J. A., 2000, "Colloidal Processing of Ceramics," *Journal of the American Ceramic Society*, Vol. 83, No. 10, pp. 2341-2359.
19. Grida, I. and J. R. G. Evans, 2003, "Extrusion Freeforming of Ceramics through Fine Nozzles," *Journal of European Ceramic Society*, Vol. 23, pp. 629-635.
20. Utela, B., R. L. Anderson and H. Kuhn, 2006, "Advanced Ceramic Materials and Three-Dimensional Printing (3DP)," *17th Solid Freeform Fabrication Symposium*, Austin, TX, pp. 290-303, pp. 290-303.
21. Yoo, J., M. J. Cima, S. Khanuja and E. M. Sachs, 1993, "Structural Ceramic Components by 3D Printing," *Solid Freeform Fabrication Symposium*, Austin, TX., pp. 40-50.
22. Cima, M. J., A. Lauder, S. Khanuja and E. Sachs, 1992, "Microstructural Elements of Components Derived from 3D Printing," *Solid Freeform Fabrication Symposium*, Austin, TX., pp. 220-227.
23. Grau, J., J. Moon, S. Uhland, M. J. Cima and E. Sachs, 1997, "High Green Density Ceramic Components Fabricated by the Slurry-Based 3DP Process," *Solid Freeform Fabrication Symposium*, Austin, TX., pp. 371-378.
24. Kernan, B. D., E. M. Sachs, M. A. Oliveira and M. J. Cima, 2003, "Three Dimensional Printing of Tungsten Carbide-Cobalt Using a Cobalt Oxide Precursor," *Solid Freeform Fabrication Symposium*, Austin, TX., pp. 616-631.
25. Moon, J., J. Grau and M. J. Cima, 2000, "Slurry Chemistry Control to Produce Easily Redispersible Ceramic Powder Compacts," *Journal of the American Ceramic Society*, Vol. 83, No. 10, pp. 2401-2408.
26. Reed, J. S., 1995, *Principles of Ceramics Processing*, John Wiley & Sons, Inc., New York.
27. Cima, M. J., J. Yoo, S. Khanuja, M. Rynerson, D. Namnour, B. Giritlioglu, J. Grau and E. M. Sachs, 1995, "Structural Ceramic Components by 3D Printing," *Solid Freeform Fabrication Symposium*, Austin, TX, pp. 479-488.
28. Beaman, J. J., J. W. Barlow, D. L. Bourell, R. H. Crawford, H. L. Marcus and K. P. McAlea, 1997, *Solid Freeform Fabrication: A New Direction in Manufacturing* Kluwer Academic Publishers, Boston, Mass.
29. Badrinarayan, B. and J. W. Barlow, 1991, "Manufacture of Injection Molds using SLS," *Solid Freeform Fabrication Symposium*, Austin, TX, pp. 245-250.
30. McNulty, T. F., F. Mohammadi, A. Bandyopadhyay, D. J. Shanefield, S. C. Danforth and A. Safari, 1998, "Development of a Binder Formulation for Fused Deposition of Ceramics," *Rapid Prototyping Journal*, Vol. 4, No. 4, pp. 144-150.
31. Greulich, M., M. Greul and T. Pintat, 1995, "Fast, Functional Prototypes via Multiphase Jet Solidification," *Rapid Prototyping Journal*, Vol. 1, No. 1, pp. 20-25.
32. King, B. H., S. Morissette, H. Denham, J. Cesarno and D. B. Dimos, 1998, "Influence of Rheology on Deposition Behavior of Ceramic Pastes in Direct Fabrication Systems," *Solid Freeform Fabrication Symposium*, Austin, TX., pp. 391-398.
33. Hinczewski, C., S. Corbel and T. Chartier, 1998, "Stereolithography for the Fabrication of Ceramic Three-Dimensional Parts," *Rapid Prototyping Journal*, Vol. 4, No. 3, pp. 104-111.
34. Cormier, D., O. Harrysson and H. West, 2004, "Characterization of H13 Steel Produced via Electron Beam Melting," *Rapid Prototyping Journal*, Vol. 10, No. 1, pp. 35-41.
35. Klocke, F. and C. Ader, 2003, "Direct Laser Sintering of Ceramics," *Solid Freeform Fabrication Symposium*, Austin, TX., pp. 447-455.
36. Kruth, J. P., L. Froyen, J. Van Vaerenbergh, P. Mercelis, M. Rombouts and B. Lauwers, 2004, "Selective Laser Melting of Iron-Based Powder," *Journal of Materials Processing Technology*, Vol. 149, Iss. 1-3, pp. 616-622.
37. Johnson, R. W., J.-H. Park, W. J. Lackey and D. W. Rosen, 2003, "Advances in Laser Chemical Vapor Deposition of Metals and Ceramics," *International Conference on Advanced Research in Virtual and Rapid Prototyping*, Leiria, Portugal.
38. Keicher, D. M., 1998, "Beyond Rapid Prototyping to Direct Fabrication: Forming Metallic Hardware Directly

- from a CAD Solid Model," *Materials Technology*, Vol. 13, No. 1, pp. 5-7.
39. Zhang, X., X. N. Jiang and C. Sun, 1999, "Microstereolithography of Polymeric and Ceramic Microstructures," *Sensors and Actuators*, Vol. 77, pp. 146-156.
40. Thomas, H. R., N. Hopkinson and P. Erasenthiran, 2007, "High Speed Sintering - Continuing Research into a New Rapid Manufacturing Process," *Solid Freeform Fabrication Symposium*, Austin, TX., pp. 682-691.
41. Das, A., G. Madras, N. Dasgupta and A. M. Umarji, 2003, "Binder Removal Studies in Ceramic Thick Shapes Made by Laminated Object Manufacturing," *Journal of the European Ceramic Society*, Vol. 23, pp. 1013-1017.
42. Blazdell, P. F., J. R. G. Evans, M. J. Edirisinghe, P. Shaw and M. J. Binstead, 1995, "The Computer Aided Manufacture of Ceramics Using Multilayer Jet Printing," *Journal of Materials Science Letters*, 14, pp. 1562-1565.
43. Slade, C. E. and J. R. G. Evans, 1998, "Freeforming Ceramics Using a Thermal Jet Printer," *Journal of Materials Science Letters*, Vol. 17, pp. 1669-1671.
44. Karlsten, R. and J. Reitan, 2003, "Metal Printing - Development of a New Rapid Manufacturing Process for Metal and Ceramic Objects," *International Conference on Advanced Research in Virtual and Rapid Prototyping*, Leiria, Portugal, pp. 569-589.
45. Solidica, Inc., 2004, "Solidica: Direct to Metal Aluminum Tooling for Advanced Manufacturing," www.solidica.com/technology.html.
46. Carrion, A., 1997, "Technology Forecast on Ink-Jet Head Technology Applications in Rapid Prototyping," *Rapid Prototyping Journal*, Vol. 3, No. 3, pp. 99-115.
47. Smay, J. E., G. M. Gratson, R. F. Shepherd, J. Cesarno and J. A. Lewis, 2002, "Directed Colloidal Assembly of 3D Periodic Structures," *Advanced Materials*, Vol. 14, No. 18, pp. 1279-1283.
48. Agarwala, M. K., V. R. Jamalabad, N. A. Langrana, A. Safari, P. J. Whalen and S. C. Danforth, 1996, "Structural Quality of Parts Processed by Fused Deposition," *Rapid Prototyping Journal*, Vol. 2, No. 4, pp. 4-19.
49. Moon, J., J. Grau, V. Knezevic, M. J. Cima and E. M. Sachs, 2002, "Ink-Jet Printing of Binders for Ceramic Components," *Journal of the American Ceramic Society*, Vol. 85, No. 4, pp. 755-762.
50. Griffith, M. L. and J. W. Halloran, 1996, "Freeform Fabrication of Ceramics via Stereolithography," *Journal of the American Ceramic Society*, Vol. 79, No. 10, pp. 2601-2608.
51. Tang, H., 2002, "Direct Laser Fusing to Form Ceramic Parts," *Rapid Prototyping Journal*, 8, 5, pp. 284-289.
52. Zhao, X., J. R. G. Evans and M. J. Edirisinghe, 2002, "Ink-Jet Printing of Ceramic Pillar Arrays," *Journal of Materials Science*, 37, pp. 1987-1992.
53. Morse, T., 1979, *Handbook of Organic Additives for Use in Ceramic Body Formulation*, Montana Energy and MHD Research and Development Institute, Butte, MT.
54. Stratasys, 2007, February 2007, "The Added Convenience of WaterWorks," http://www.stratasys.com/systems_misc.aspx?id=132.
55. Mott, M., J. H. Song and J. R. G. Evans, 1999, "Microengineering of Ceramics by Direct Ink-Jet Printing," *Journal of the American Ceramic Society*, Vol. 82, No. 7, pp. 1653-1658.
56. Crane, N. B., J. Wilkes, E. Sachs and S. M. Allen, 2006, "Improving Accuracy of Powder-Based SFF Processes by Metal Deposition from a Nanoparticle Dispersion," *Rapid Prototyping Journal*, Vol. 12, No. 5, pp. 266-274.